Technical Report DIKU-TR-98/10
Department of Computer Science
University of Copenhagen
Universitetsparken 1
2100 Copenhagen
Denmark

submitted for publication
May 1998

Efficient Image Segmentation Using Partial Differential Equations and Morphology

Joachim Weickert

Department of Computer Science, University of Copenhagen, Universitetsparken 1, 2100 Copenhagen, Denmark
E-mail: joachim@diku.dk

Abstract

The goal of this paper is to present segmentation algorithms which combine regularization by nonlinear partial differential equations (PDEs) with a watershed transformation with region merging. We develop efficient algorithms for two well-founded PDE methods. They use an additive operator splitting (AOS) leading to recursive and separable filters. Further speed-up can be obtained by embedding AOS schemes into a pyramid framework. Examples are presented which demonstrate that the preprocessing by these PDE techniques eases and stabilizes the segmentation. The typical CPU time for segmenting a 256^2 image on a workstation is less than 2 seconds.

Key Words: Nonlinear diffusion, additive operator splitting, Gaussian pyramid, watershed segmentation, region merging

CR Subject Classification: I.4.6, I.4.3, I.4.4.

1 Introduction

Segmentation is one of the bottlenecks of many image analysis and computer vision tasks ranging from medical image processing to robot navigation. Ideally it should be efficient to compute and correspond well with the physical objects depicted in the image.
In the last decade much research on PDE-based regularization methods has been carried out, see e.g. [1, 2] for an overview. Although the impressive results suggest that they might be attractive as a preprocessing step for many subsequent image analysis methods, little research has been carried out which combines PDE-based preprocessing methods with other techniques.
In the present paper we address this topic by combining two efficient PDE-based regularization methods with a watershed algorithm, a simple morphological technique for image segmentation.
This leads to segmentation algorithms which can be generalized in a straightforward way to arbitrary dimensional data sets. Their complexity is linear in the pixel number, and they produce identical results if the image is rotated by 90 degrees. An overall CPU time of less than 2 seconds for segmenting a 256^2 image on a workstation makes them attractive for many time-critical applications.

The paper is organized as follows. Section 2 sketches the basic ideas behind two well-posed PDE-based regularization methods: a contrast-enhancing nonlinear diffusion filter and a diffusion reaction-method with a similarity term. In Section 3 we develop efficient and reliable numerical techniques for these methods. They are based on an additive operator splitting (AOS). For approximating the diffusion-reaction method, these AOS techniques are embedded into a pyramid framework. In Section 4 we discuss the watershed algorithm with region merging, and in Section 5 we illustrate the usefulness of the combined segmentation process by applying it to several examples. The paper is concluded with a summary in Section 6.

Related work. The work presented here has been influenced by several related approaches. Closest in terms of efficient PDE-based regularization methods is the work of Acton [3] on multigrid versions for nonlinear diffusion filtering. They are, however not based on AOS schemes and they do not use methods with a reaction term. It is common to supplement watershed segmentations with tools for reducing the oversegmentation problem. An algorithm by Orphanoudakis *et al.* [4] also uses region merging for this purpose, but it applies statistical instead of PDE-based smoothing strategies. Promising results of combining watershed algorithms with nonlinear diffusion have been described recently by De Vleeschauer *et al.* [5] and Sijbers *et al.* [6]. Investigations of watershed algorithms within scale-space hierarchies have been carried out by Griffin *et al.* [7] and Olsen [8] for the linear diffusion scale-space and by Jackway [9] for the dilation–erosion scale-space. A nonmorphological segmentation algorithm based on nonlinear diffusion scale-spaces has been studied by Niessen *et al.* [10, 11]. This discussion shows that the novelty of our approach consist of using efficient PDE-based regularization strategies such as pyramid AOS in combination with a classical morphological segmentation tool, the watershed algorithm. This results in a fast segmentation tool.

2 PDE-Based Regularization

Below two prototypes for well-posed PDE-based regularization techniques are presented. The first one allows contrast enhancement, while the second one can be related to energy minimization methods. These two methods are only representatives of a much larger class of diffusion-based smoothing methods. For a more detailed treatment of this topic the reader is referred to [2].

2.1 The Nonlinear Diffusion Filter of Catté *et al.*

In the m-dimensional case the filter of Catté, Lions, Morel and Coll [12] has the following structure:
Let $\Omega := (0, a_1) \times .... \times (0, a_m)$ be our image domain and consider a (scalar) image $f(x)$ as a bounded mapping from Ω into the real numbers $\mathbb{R}$. Then a filtered image $u(x,t)$ of $f(x)$ is calculated by solving the diffusion equation with the original image as initial state, and reflecting boundary conditions:

$$\partial_t u = \sum_{l=1}^{m} \partial_{x_l}\Big(g(|\nabla u_\sigma|^2)\, \partial_{x_l} u\Big) \tag{1}$$

$$u(x,0) = f(x), \tag{2}$$

$$\partial_n u|_{\partial\Omega} = 0, \tag{3}$$

where n denotes the normal to the image boundary $\partial\Omega$.
The "time" t is a scale parameter: larger values lead to simpler image representations. In order to reduce smoothing at edges, the diffusivity g is chosen as a decreasing function of the edge detector $|\nabla u_\sigma|$, where ∇u_σ is the gradient of a Gaussian-smoothed version of u:

$$\nabla u_\sigma := \nabla(K_\sigma * u), \tag{4}$$

$$K_\sigma := \frac{1}{(2\pi\sigma^2)^{m/2}} \exp\left(-\frac{|x|^2}{2\sigma^2}\right). \tag{5}$$

We use the diffusivity

$$g(s^2) := \begin{cases} 1 & (s^2 = 0) \\ 1 - \exp\left(\frac{-3.315}{(s/\lambda)^8}\right) & (s^2 > 0). \end{cases} \tag{6}$$

For such rapidly decreasing diffusivities, smoothing on both sides of an edge is much stronger than smoothing across it. This selective smoothing process prefers intraregional smoothing to interregional blurring. The factor 3.315 ensures that the flux $\Phi(s) := sg(s)$ is increasing for $|s| \leq \lambda$ and decreasing for $|s| > \lambda$. Thus, λ is a contrast parameter separating low-contrast regions with (smoothing) forward diffusion from high-contrast locations where backward diffusion may enhance edges [13]. After some time this filter creates segmentation-like results which are piecewise almost constant. For $t \to \infty$, however, the image becomes completely flat [2]. Well-posedness results for this filter can be found in [12, 2] and a scale-space interpretation in terms of an extremum principle as well as decreasing variance, decreasing energy, and increasing entropy is given in [2].

2.2 A Diffusion-Reaction Filter

Diffusion filters with a constant steady-state require to specify a stopping time T, if one wants to get nontrivial results. Sometimes it is attempted to circumvent this task by adding an additional reaction term which keeps the steady-state solution close to the original image:

$$\partial_t u = \operatorname{div}\left(g(|\nabla u|^2)\,\nabla u\right) + \beta(f-u) \qquad (\beta > 0). \tag{7}$$

This equation can be regarded as the descent method of the energy functional

$$E_f(u) := \int_\Omega \left(\tfrac{\beta}{2}\cdot(u-f)^2 \,+\, \Psi(|\nabla u|)\right) dx, \tag{8}$$

with a potential function $\Psi(|\nabla u|)$ whose gradient is given by

$$\nabla\Big(\Psi(|\nabla u|)\Big) \,=\, g(|\nabla u|^2)\nabla u. \tag{9}$$

The first term in the integrand of the energy functional is a similarity term which causes the regularized image to be close to the original one, while the second term tends to increase its smoothness.
It should be noted that the reaction term $\beta(f-u)$ shifts the problem of specifying a stopping time T to the problem of determining β; so it appears to be a matter of taste which formulation is preferred.
From a theoretical viewpoint, it is advantageous to choose a convex potential function Ψ, since this guarantees well-posedness and stable algorithms [14]. For nonconvex potentials as in [15], several well-posedness questions are open. An example for a diffusivity leading to a convex potential is [16]

$$g(|\nabla u|^2) := \frac{1}{\sqrt{1+|\nabla u|^2/\lambda^2}} \qquad (\lambda > 0). \tag{10}$$

3 Efficient Algorithms for PDE-Based Regularization

3.1 Limitations of Conventional Schemes

Let us first consider finite difference approximations to the m-dimensional diffusion filter of Catté *et al.*.
A discrete m-dimensional image can be regarded as a vector $f \in \mathbb{R}^N$, whose components f_i, $i \in \{1,...,N\}$ display the grey values at the pixels. Pixel i represents the location x_i. Let h_l denote the grid size in the l direction. We consider discrete times $t_k := k\tau$, where $k \in \mathbb{N}_0$ and τ is the time step size. By u_i^k and g_i^k we denote approximations to $u(x_i,t_k)$ and $g(|\nabla u_\sigma(x_i,t_k)|^2)$, respectively, where the gradient is replaced by central differences.
The simplest discretization of the diffusion equation with reflecting boundary conditions is given by

$$\frac{u_i^{k+1}-u_i^k}{\tau} \,=\, \sum_{l=1}^{m}\sum_{j\in\mathcal{N}_l(i)} \frac{g_j^k+g_i^k}{2h_l^2}\,(u_j^k-u_i^k). \tag{11}$$

where $\mathcal{N}_l(i)$ consists of the two neighbours of pixel i along the l direction (boundary pixels may have only one neighbour). In vector–matrix notation this becomes

$$\frac{u^{k+1} - u^k}{\tau} \;=\; \sum_{l=1}^{m} A_l(u^k)\, u^k. \tag{12}$$

A_l describes the diffusive interaction in l direction. One can calculate u^{k+1} directly (explicitly) from u^k without any matrix inversion:

$$u^{k+1} \;=\; \Big(I + \tau \sum_{l=1}^{m} A_l(u^k)\Big)\, u^k. \tag{13}$$

For this reason it is called *explicit scheme*. Each explicit iteration step can be performed very fast, but the step size has to be very small: one can show [17] that in order to guarantee stability, the step size must satisfy

$$\tau \;\leq\; \frac{1}{\sum_{l=1}^{m} \frac{2}{h_l^2}}. \tag{14}$$

For most practical applications, this restriction requires to use a very high number of iterations, such that the explicit scheme is rather slow.
Thus, we consider a slightly more complicated discretization next, namely

$$\frac{u^{k+1} - u^k}{\tau} \;=\; \sum_{l=1}^{m} A_l(u^k)\, u^{k+1}. \tag{15}$$

This scheme does not give the solution u^{k+1} directly (explicitly): It requires to solve a linear system first. It is called a *linear-implicit (semi-implicit)* scheme. The solution u^{k+1} is given by

$$u^{k+1} \;=\; \Big(I - \tau \sum_{l=1}^{m} A_l(u^k)\Big)^{-1} u^k. \tag{16}$$

This scheme is absolutely stable [2].
In the 1-D case the system matrix is tridiagonal and diagonally dominant. For such a system a Gaussian algorithm for tridiagonal systems (also called *Thomas algorithm*) solves the problem in linear complexity.
For dimensions $m \geq 2$, however, it is not possible to order the pixels in such a way that in the i-th row all nonvanishing elements of the system matrix can be found within the positions $[i, i-m]$ to $[i, i+m]$: Usually, the matrix reveals a much larger bandwidth. Applying direct algorithms such as Gaussian elimination would destroy the zeros within the band and would lead to an immense storage and computation effort. Typical iterative algorithms become slow for large τ, since this increases the condition number of the system matrix. Thus, in spite of its absolute stability, the semi-implicit scheme is often not much faster than the explicit one.

3.2 AOS Schemes

In order to address the preceding problem we consider a modification of (16), namely the *additive operator splitting (AOS) scheme*

$$u^{k+1} \;=\; \frac{1}{m} \sum_{l=1}^{m} \Big(I - m\tau A_l(u^k)\Big)^{-1} u^k. \tag{17}$$

The operators $B_l(u^k) := I - m\tau A_l(u^k)$ describe one-dimensional diffusion processes along the x_l axes. Under a consecutive pixel numbering along the direction l they come down to strictly diagonally dominant tridiagonal matrices which can be efficiently inverted by the Thomas algorithm.
Moreover, (17) has the same first-order Taylor expansion in τ as the explicit and semi-implicit scheme: all methods are $O(\tau + h_1^2 + ... + h_m^2)$ approximations to the continuous equation.
Since it is an *additive* splitting, all coordinate axes are treated in exactly the same manner. This is in contrast to conventional splitting techniques from the literature, which are *multiplicative* [18]. They may produce different results if the image is rotated by 90 degrees.
Recently a general framework for discrete nonlinear diffusion scale-spaces has been discovered, which guarantees that the discretization reveals the same scale-space properties as its continuous counterpart [2]. One can verify [17] that the AOS scheme creates such a discrete nonlinear diffusion scale-space for every (!) step size τ. As a consequence, it preserves the average grey level μ, satisfies a causality property in terms of a maximum–minimum principle, and converges to a constant steady state. Moreover, the process is a simplifying, information-reducing transform with respect to many aspects: The p-norms

$$\|u^k\|_p := (\sum_{i=1}^{N} |u_i^k|^p)^{1/p} \tag{18}$$

and all even central moments

$$M_{2n}[u^k] := \frac{1}{N} \sum_{j=1}^{N} (u_j^k - \mu)^{2n} \tag{19}$$

are decreasing in k, and the entropy

$$S[u^k] := -\sum_{j=1}^{N} u_j^k \ln u_j^k, \tag{20}$$

a measure of uncertainty and missing information, is increasing in k (if f_j is positive for all j).
Table 1 summarizes the features of the discussed schemes. Full algorithmic details of AOS schemes can be found in [17], and a parallel implementation for processing 3-D images is described in [19].
Many nonlinear diffusion problems require only the elimination of noise and some small-scale details. Usually this can be accomplished with less than 10 iterations in sufficient precision. On an HP 9000/889 workstation, this takes about 1 second for a 256^2 image.

3.3 Pyramid AOS

The diffusion-reaction method (7) requires to find the steady-state of the process. Even with large time step sizes, the diffusion process will mainly act within a fairly small vicinity around each pixel. Thus, many iterations are required if the image size is large. In order to speed up the process, we may embed the AOS schemes into a pyramid framework. The idea is as follows:

Table 1: Schemes which create discrete nonlinear diffusion scale-spaces.

scheme	formula	stability	costs/iter.	efficiency
explicit	$u^{k+1} = \left(I + \tau \sum_{l=1}^{m} A_l(u^k)\right) u^k$	$\tau \leq \frac{1}{\sum_{l=1}^{m} \frac{2}{h_l^2}}$	very low	low
semi-implicit	$u^{k+1} = \left(I - \tau \sum_{l=1}^{m} A_l(u^k)\right)^{-1} u^k$	$\tau < \infty$	high	fair
AOS	$u^{k+1} = \frac{1}{m} \sum_{l=1}^{m} \left(I - m\tau A_l(u^k)\right)^{-1} u^k$	$\tau < \infty$	low	high

- downsample the image by creating a Gaussian pyramid [20] with the smoothing mask $(\frac{1}{4}, \frac{1}{2}, \frac{1}{4})$
- adapt the filter parameters to the downsampled image; experiments have shown that λ should be divided by 1.5 and β by 4 if one reduces the image size by a factor 2.
- start with the coarsest level (e.g. a 4×4 image), and apply AOS iterations until convergence is obtained.
- expand this solution to the next finer level by linear interpolation, and use it as initial value for AOS iterations at this level.
- proceed in the same way until convergence at the finest level is reached.

Figure 1 illustrates the effect of pyramid AOS. Typically, only a few iterations (around 10) are necessary in order to obtain good convergence at each level. Since the Gaussian pyramid decomposition can be performed with linear complexity, the overall complexity remains linear as well. For regularizing a 256^2 image on an HP 9000/889 workstation, a CPU time of 1–1.5 seconds is sufficient.

4 Watershed Segmentation with Region Merging

The previously discussed PDE-based regularization techniques lead to piecewise almost constant images with less noise and less fine-scale details.
In order to create a true segmentation, we have to postprocess the regularized image by a technique which gives an edge map without dangling edges. This edge map should lead to a partitioning of the entire image into a finite number of regions, it should handle the semantically important corners and junctions gracefully, and – last but not least – it should be fast.
We found a watershed technique [21, 22, 23] based on the gradient magnitude very useful for these purposes. Such a technique regards an image as a landscape where the intensity values correspond to the elevation. Areas where a rain drop would drain to the same minimum are denoted as catchment basins, and the lines separating adjacent catchment basins are called watersheds. Watersheds are a morphological technique, since they are invariant under monotone grey scale-transformations. They lead to an

Figure 1: TOP: Gaussian pyramid of a test image. BOTTOM: Regularized by pyramid AOS.

image segmentation into regions, and they can describe edge junctions [24]. This is in contrast to edge detectors based on zero-crossings of differential operators: they do not allow to detect T-junctions [25].

We used an implementation as proposed by Fairfield [26]. The basic idea of this algorithm is sliding downhill on the gradient squared surface until one arrives at a local minimum. Then one replaces all pixels along this path by the image intensity at its corresponding extremum. This algorithm has linear complexity.

Watershed algorithms often create too many segments. Although this oversegmentation is less dominant in the PDE-regularized image than in the original one, it may still lead to problems. Numerous ways are described in order to deal with the oversegmentation problem, for instance by using markers [23, 27], region merging [28, 29, 4], or scale-space techniques [7, 9, 8]. In our case we shall see that a simple region merging strategy is adequate.

In such a step, adjacent regions are merged if their contrast difference is below a specified threshold. This contrast parameter can be related to the contrast parameter λ of the PDE-based regularization, thus it does not constitute an additional parameter.

Finding a connected region where neighbouring pixels do not differ by more than a specified contrast value can be performed in linear complexity and the result is independent of the order in which the algorithm runs through the pixels. Thus, the entire segmentation algorithm is invariant under image rotations by 90 degrees and it reveals a linear total complexity.
A watershed segmentation of a 256^2 image with subsequent region merging takes about 0.5 CPU seconds on an HP 9000/889. Thus, the overall segmentation time including the PDE-based regularization is less than 2 seconds.

5 Experiments

Figure 2 illustrates how preprocessing by nonlinear diffusion filtering greatly reduces the number of segments in a medical MR image. We also observe that under nonlinear diffusion the segment boundaries remain well located and need not be traced back in order to improve their localization. As can be seen for instance at the cerebellum, the segments correspond well with the depicted physical objects. Moreover, segmentation of elongated objects does not create any problem.
In Figure 3 it is shown that the merging step can be essential for avoiding the over-segmentation problems in the watershed algorithm. Nonlinear diffusion may create almost piecewise constant areas, but small fluctuations within such an area introduce many semantically irrelevant catchment basins. Such fluctuations can also be caused by quantization errors, e.g. by storing grey values in a bytewise manner. Merging adjacent regions with similar grey values constitutes a simple remedy for these problems.
Finally, Figure 4 gives a comparison between the two PDE-based regularization techniques. The diffusion-reaction method gives smoother results and is better capable of eliminating small-scale structures, while the pure nonlinear diffusion process is advantageous for recovering elongated structures. It leads to a very realistic segmentation of the man walking along the hallway.

6 Summary

We have presented efficient algorithms for two prototypes for PDE-based regularization techniques. These regularizations greatly simplify subsequent segmentation tasks, such that already a simple watershed algorithm with region merging gives good results. Thanks to the AOS and pyramid AOS schemes these segmentation techniques are very fast. This makes them attractive for many time-critical applications. All axes are treated equally, since the result is independent of the pixel ordering. The entire algorithm can be extended in a straightforward way to m-dimensional data, and the linear complexity in the pixel number remains valid in any dimension.

Acknowledgements. This work has been carried out within the EU-TMR network VIRGO. The author thanks Ole Fogh Olsen and Mads Nielsen for providing the hallway image. The watershed algorithm is a modification of an implementation by Hans Oltmans.

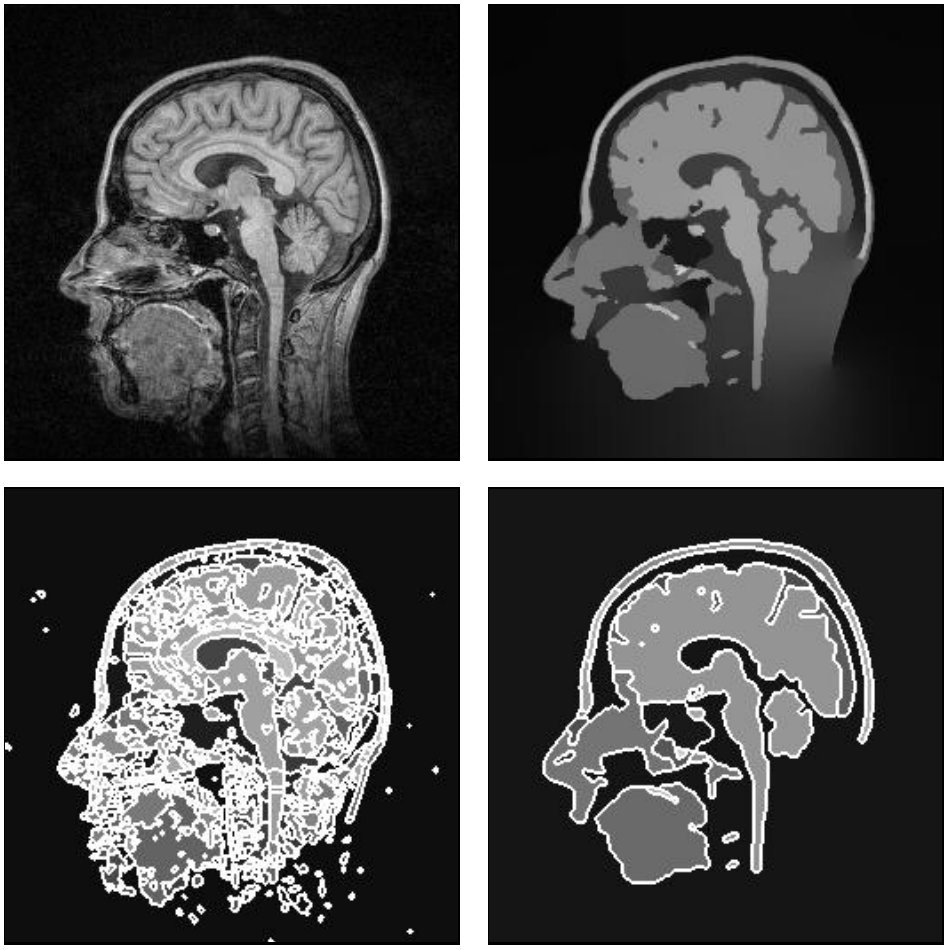

Figure 2: TOP LEFT: Test image. TOP RIGHT: Filtered by isotropic nonlinear diffusion. BOTTOM LEFT: Segmented. BOTTOM RIGHT: Diffused and segmented.

References

[1] B.M. ter Haar Romeny (Ed.), *Geometry-driven diffusion in computer vision*, Kluwer, Dordrecht, 1994.

[2] J. Weickert, *Anisotropic diffusion in image processing*, ECMI Series, Teubner-Verlag, Stuttgart, 1998.

[3] S.T. Acton, *Multigrid anisotropic diffusion*, IEEE Trans. Image Proc., Vol. 7, 280–291, 1998.

[4] S.C. Orphanoudakis, G. Tziritas, K. Haris, *A hybrid algorithm for the segmentation of 2D and 3D medical images*, Y. Bizais, C. Barillot, R. Di Paola (Eds.), Information processing in medical imaging, Kluwer, Dordrecht, 385–386, 1995.

[5] D. De Vleeschauer, F.A. Cheikh, R. Hamila, M. Gabbouj, *Watershed segmentation of an image enhanced by Teager energy driven diffusion*, Proc. Sixth Int. Conf. on Image Processing and its Applications (IPA '97, Dublin, July 1997), 254–258, 1997.

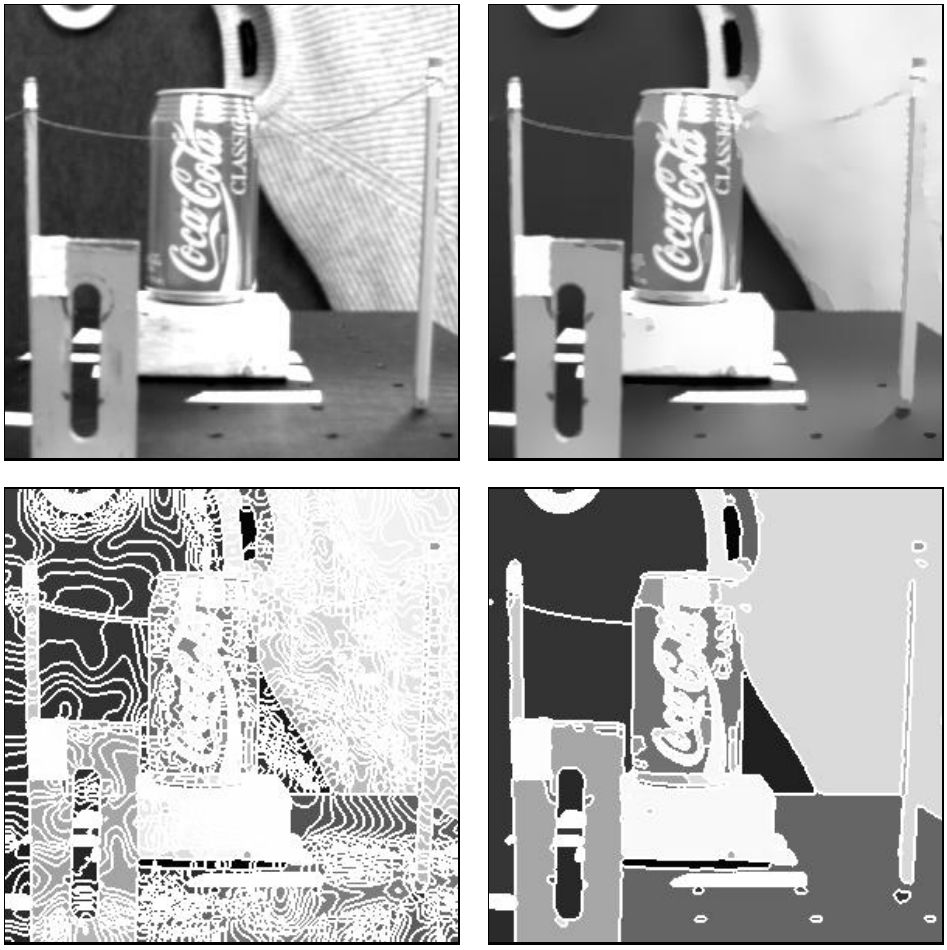

Figure 3: TOP LEFT: Test image. TOP RIGHT: Filtered by nonlinear diffusion. BOTTOM LEFT: Diffused, segmented without merging. BOTTOM RIGHT: Diffused, segmented with merging.

[6] J. Sijbers, P. Scheunders, M. Verhoye, A. Van der Linden, D. Van Dyck, E. Raman, *Watershed-based segmentation of 3D MR data for volume quantization*, Magnetic Resonance Imaging, Vol. 15, 679–688, 1997.

[7] L.D. Griffin, A.C.F. Colchester, G.P. Robinson, *Scale and segmentation of grey-level images using maximum gradient paths*, Image and Vision Computing, Vol. 10, 389–402, 1992.

[8] O.F. Olsen, *Multiscale watershed segmentation*, J. Sporring, M. Nielsen, L. Florack, P. Johansen (Eds.), Gaussian scale-space theory, Kluwer, Dordrecht, 191–200, 1997.

[9] P.T. Jackway, *Gradient watersheds in morphological scale-space*, IEEE Trans. Image Proc., Vol. 5, 913–921, 1996.

[10] W.J. Niessen, K.L. Vincken, J. Weickert, M.A. Viergever, *Nonlinear multiscale representations for image segmentation*, Computer Vision and Image Understanding, Vol. 66, 233–245, 1997.

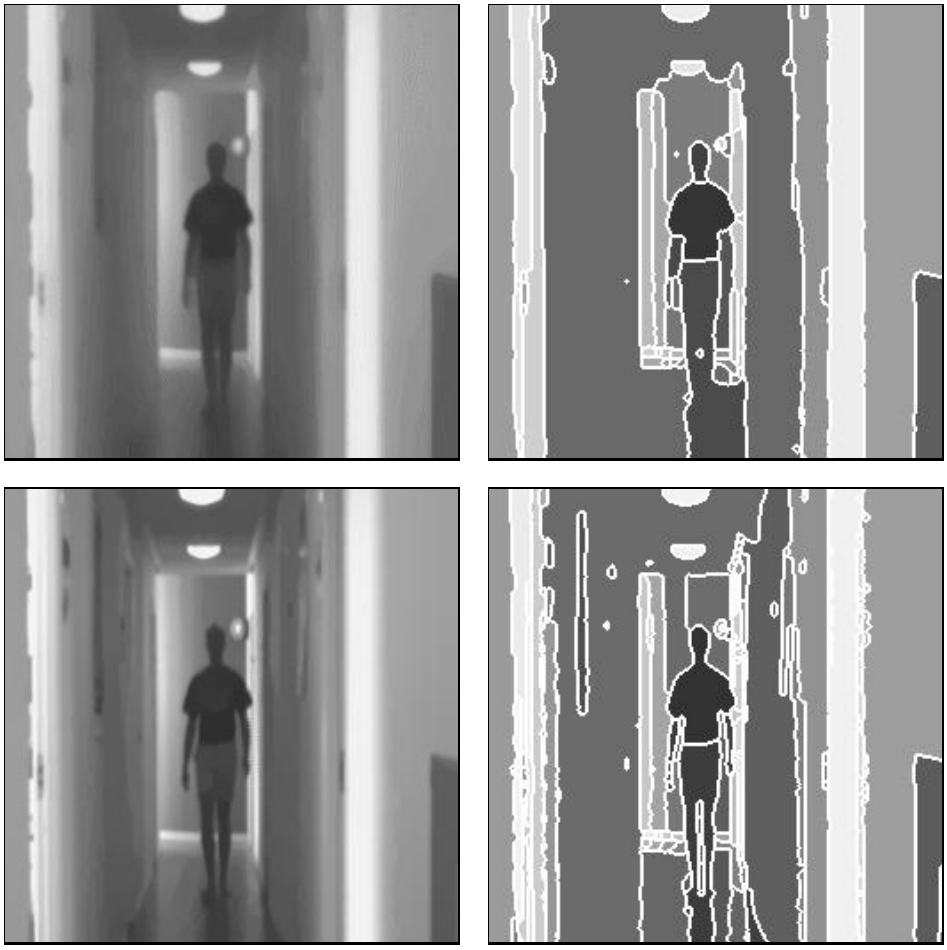

Figure 4: Hallway scene. TOP LEFT: Regularized by diffusion–reaction. TOP RIGHT: Diffusion–reaction, segmented. BOTTOM LEFT: Diffusion. BOTTOM RIGHT: Diffusion, segmented.

[11] W.J. Niessen, K.L. Vincken, J. Weickert, M.A. Viergever, *Three-dimensional MR brain segmentation*, Proc. Sixth Int. Conf. on Computer Vision (ICCV '98, Bombay, Jan. 4–7, 1998), 53–58, 1998.

[12] F. Catté, P.-L. Lions, J.-M. Morel, T. Coll, *Image selective smoothing and edge detection by nonlinear diffusion*, SIAM J. Numer. Anal., Vol. 29, 182–193, 1992.

[13] P. Perona, J. Malik, *Scale space and edge detection using anisotropic diffusion*, IEEE Trans. Pattern Anal. Mach. Intell., Vol. 12, 629–639, 1990.

[14] C. Schnörr, *Unique reconstruction of piecewise smooth images by minimizing strictly convex non-quadratic functionals*, J. Math. Imag. Vision, Vol. 4, 189–198, 1994.

[15] N. Nordström, *Biased anisotropic diffusion - a unified regularization and diffusion approach to edge detection*, Image and Vision Computing, Vol. 8, 318–327, 1990.

[16] P. Charbonnier, L. Blanc–Féraud, G. Aubert, M. Barlaud, *Two deterministic half-quadratic regularization algorithms for computed imaging*, Proc. IEEE Int. Conf. Image Processing (ICIP–94, Austin, Nov. 13–16, 1994), Vol. 2, IEEE Computer Society Press, Los Alamitos, 168–172, 1994.

[17] J. Weickert, B.M. ter Haar Romeny, M.A. Viergever, *Efficient and reliable schemes for nonlinear diffusion filtering*, IEEE Trans. Image Proc., Vol. 7, 398–410, 1998.

[18] G.I. Marchuk, *Splitting and alternating direction methods*, P.G. Ciarlet, J.-L. Lions (Eds.), Handbook of numerical analysis, Vol. I, 197–462, North Holland, Amsterdam, 1990.

[19] J. Weickert, K.J. Zuiderveld, B.M. ter Haar Romeny, W.J. Niessen, *Parallel implementations of AOS schemes: A fast way of nonlinear diffusion filtering*, Proc. 1997 IEEE International Conference on Image Processing (ICIP–97, Santa Barbara, Oct. 26–29, 1997), Vol 3., 396–399, 1997.

[20] P.J. Burt, E.H. Adelson, *The Laplacian pyramid as a compact image code*, IEEE Trans. Comm., Vol. 31, 532–540, 1983.

[21] H. Digabel, C. Lantuéjoul, *Iterative algorithms*, J.L. Chermant (Ed.), Proc. Second Europ. Symp. on Quantitative Analysis of Microstructures in Material Science, Biology and Medicine, Dr.-Riederer-Verlag, Stuttgart, 85–99, 1977.

[22] S. Beucher, C. Lantuéjoul, *Use of watersheds in contour detection*, Proc. Int. Workshop on Image Processing, Real-Time Edge and Motion Detection/Estimation (Rennes, Sept. 17–21, 1979), IRISA Report No. 131, 2.1–2.12, 1979.

[23] F. Meyer, S. Beucher, *Morphological segmentation*, J. Vis. Comm. Image Repr., Vol. 1, 21–46, 1990.

[24] L. Najman, M. Schmitt, *Watershed of a continuous function*, Signal Processing, Vol. 38, 99–112, 1994.

[25] V. Torre, T.A. Poggio, *On edge detection*, IEEE Trans. Pattern Anal. Mach. Intell., Vol. 8, 148–163, 1986.

[26] J. Fairfield, *Toboggan contrast enhancement for contrast segmentation*, Proc. 10th Int. Conf. Pattern Recognition (ICPR 10, Atlantic City, June 16–21, 1990), IEEE Computer Society Press, Los Alamitos, Vol. 1, 712–716, 1990.

[27] L. Najman, M. Schmitt, *Geodesic saliency of watershed contours and hierarchical segmentation*, IEEE Trans. Pattern Anal. Mach. Intell., Vol. 18, 1163–1173, 1996.

[28] L. Vincent, P. Soille, *Watersheds in digital spaces: An efficient algorithm based on immersion simulation*, IEEE Trans. Pattern Anal. Mach. Intell., Vol. 13, 583–589, 1991.

[29] F. Maes, D. Vandermeulen, P. Suetens, G. Marchal, *Computer-aided interactive object delineation using an intelligent paintbrush technique*, N. Ayache (Ed.), Computer vision, virtual reality and robotics in medicine, Lecture Notes in Computer Science, Vol. 905, Springer, Berlin, 77–83, 1995.